doi:10.1093/jmcb/mjz105
Published online November 19, 2019

Article

Protective effects of human umbilical cord mesenchymal stem cell-derived conditioned medium on ovarian damage

Liming Hong[1,†], Long Yan[2,†], Zhimin Xin[1], Jie Hao[2], Wenjing Liu[2], Shuyu Wang[1], Shujie Liao[3], Hongmei Wang[2,*], and Xiaokui Yang[1,*]

[1] Department of Human Reproductive Medicine, Beijing Obstetrics and Gynecology Hospital, Capital Medical University, Beijing 100026, China
[2] State Key Laboratory of Stem Cell and Reproductive Biology, Institute of Zoology, Chinese Academy of Sciences, Beijing 100101, China
[3] Department of Gynaecology and Obstetrics, Reproductive Medical Center, Tongji Hospital, Tongji Medical College, Huazhong University of Science and Technology, Wuhan 430030, China
[†] These authors contributed equally to this work.
[*] Correspondence to: Xiaokui Yang, E-mail: xiaokuiyang2012@163.com; Hongmei Wang, E-mail: wanghm@ioz.ac.cn

Edited by Anming Meng

Chemotherapeutic agents are extensively used to treat malignancies. However, chemotherapy-induced ovarian damage and reduced fertility are severe side effects. Recently, stem cell transplantation has been reported to be an effective strategy for premature ovarian insufficiency (POI) treatment, but safety can still be an issue in stem cell-based therapy. Here, we show the protective effects of human umbilical cord mesenchymal stem cell-derived conditioned medium (hUCMSC-CM) on a cisplatin (Cs)-induced ovarian injury model. hUCMSC-CM can relieve Cs-induced depletion of follicles and preserve fertility. In addition, hUCMSC-CM can decrease apoptosis of oocytes and granulosa cells induced by Cs. RNA sequencing analysis reveals the differentially expressed genes of ovaries after Cs and hUCMSC-CM treatments, including genes involved in cell apoptosis. Furthermore, we show that the granulocyte colony-stimulating factor (G-CSF)/phosphatidylinositol 3-kinase (PI3K)/protein kinase B (Akt) pathway plays an important role in protecting granulosa cells from Cs-induced apoptosis. Together, we confirm the protective effects of hUCMSC-CM on ovarian reserve and fertility in mice treated with Cs, highlighting the remarkable therapeutic effects of hUCMSC-CM.

Keywords: stem cell, ovarian damage, RNA sequencing

Introduction

Premature ovarian insufficiency (POI) and infertility are common and severe side effects of chemotherapy (Letourneau et al., 2012). Chemotherapeutic agents target oocytes directly or induce oocyte death indirectly by damaging somatic cells (Morgan et al., 2012). Currently, several therapeutic methods have been used to improve fertility and alleviate the complications caused by low estrogen, such as hormone replacement therapy (HRT), ovarian tissue cryopreservation, and gonadotropin-releasing hormone (GnRH) agonist administration. However, these methods do not fundamentally improve ovarian function. HRT is an effective treatment for symptoms associated with low estrogen levels in women with POI, but it does not improve fertility (Sassarini et al., 2015; Webber et al., 2016). Cryopreservation of oocytes and ovarian tissue is a good option for preserving fertility, but the method does not maintain ovarian function for an extended period (Anderson and Wallace, 2011; Donnez and Dolmans, 2011). The administration of GnRH agonists has been investigated as a potential strategy for a long time (Waxman et al., 1987), and a large randomized multi-center clinical trial reported a significant reduction in chemotherapy-induced ovarian failure when GnRH-a was administered (Del et al., 2011). However, the protective effects of GnRH agonists remain controversial (Gerber et al., 2011). Additionally, the c-Abl kinase inhibitor imatinib, sphingosine-based lipid signaling molecule sphingosine-1-phosphate (SIP), and luteinizing hormone (LH) are reported to prevent premature infertility (Morita and Tilly, 2000; Gonfloni et al., 2009; Rossi et al., 2017). The fertoprotective effects of these approaches require further confirmation. Meanwhile, more effective options to protect both fertility and

Received January 27, 2019. Revised August 31, 2019. Accepted September 15, 2019.

endocrine function are expected to be discovered in the near future.

Recently, stem cell transplantation has been shown to be a new strategy for the treatment of POI and infertility (Volarevic et al., 2014; Sheikhansari et al., 2018). Based on accumulating evidence, stem cells improve the ovarian function due to their paracrine effects rather than differentiating into specific cells (Wang et al., 2017; Li et al., 2017; Khanmohammadi et al., 2018). Studies on stem cell-derived secreted factors report that the secretome, microvesicles, and exosome are present in the medium where stem cells were cultured, which is known as conditioned medium (CM) (Kim et al., 2013a; Sdrimas and Kourembanas, 2014; Phinney and Pittenger, 2017). The contents of these vesicles secreted by mesenchymal stem cells (MSCs) include cytokines and growth factors, signaling lipids, messenger RNAs (mRNAs), and regulatory miRNAs (Phinney and Pittenger, 2017; Zhang et al., 2017). These factors are involved in cell–cell communication, cell signaling, and alteration of cell or tissue metabolism. CM could promote tissue/organ repair under various conditions (Pawitan, 2014). In addition, CM has several advantages compared with stem cells. (i) CM can be manufactured, freeze-dried, packaged, and transported more easily (Pawitan, 2014); (ii) it eliminates issues with matching the donor and the recipient to avoid rejection problems (Pawitan, 2014); and (iii) it eliminates the potential side effects of stem cells on tumor cells, such as differentiating into other stromal cells types, increasing the metastatic abilities of tumor cells, and stimulating the epithelial–mesenchymal transition of tumor cells (Mohr and Zwacka, 2018). Based on the superiority of MSC-derived CM, in the present study, we investigate the role of human umbilical cord mesenchymal stem cell-derived CM (hUCMSC-CM) on ovarian damage induced by cisplatin (Cs) and the mechanisms underlying the protective effects.

hUCMSC-CM can exert protective effects on frozen and thawed ovarian tissues compared with the serum-free culture medium (Jia et al., 2017). In the present study, we have confirmed the protective effects of hUCMSC-CM on ovarian damage induced by Cs. RNA sequencing (RNA-Seq) is applied to compare the differentially expressed genes after Cs and hUCMSC-CM treatments and identify the initial factors mediating the protective effects of hUCMSC-CM. Our results have indicated that hUCMSC-CM can protect ovaries from Cs-induced damage, and the granulocyte colony-stimulating factor (G-CSF)/phosphatidylinositol 3-kinase (PI3K)/protein kinase B (Akt) pathway plays an important role in protecting granulosa cells from apoptosis.

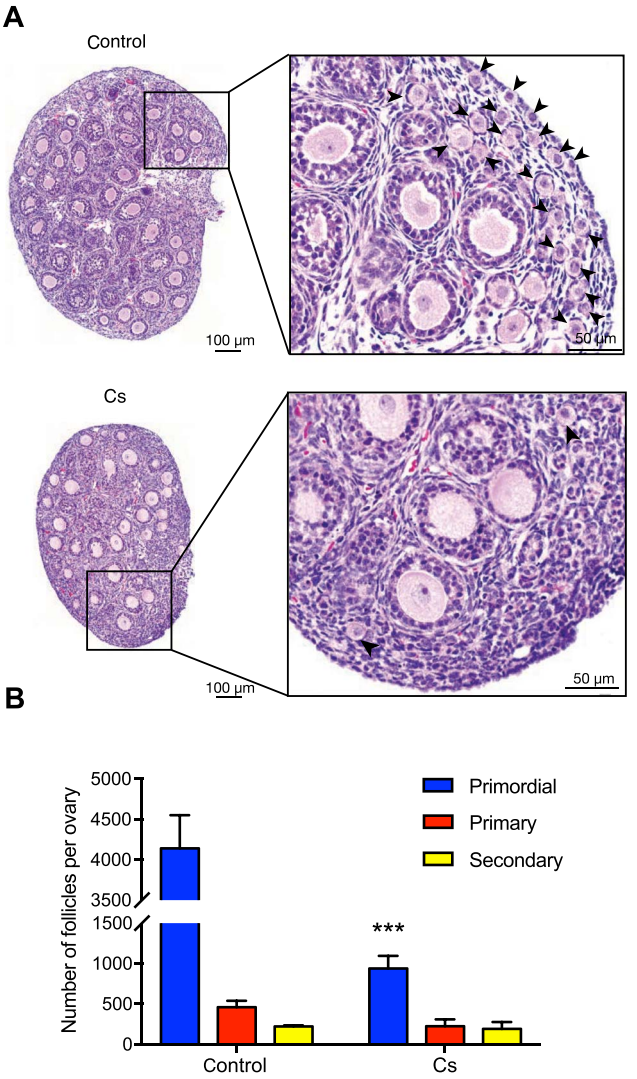

Figure 1 Cs induces a significant decrease of primordial follicles. (**A**) H&E staining of ovaries. H&E-stained ovary sections were obtained from P9 mice. Mice were injected with a single dose of Cs (5 mg/kg body weight) or 0.9% NaCl at P5. Black arrowheads indicate the primordial follicles. (**B**) Quantification of the numbers of primordial, primary, and secondary follicles. Data are presented as mean ± SD ($n = 6$). ***$P < 0.001$.

Results

Cs induces a significant decrease of primordial follicles

To investigate the protective role of hUCMSC-CM on ovarian damage, first of all, we established an ovarian injury model on postnatal day 5 (P5) mice. Previously, Kim et al. (2013b) reported that primordial and primary follicles are the predominant structures in P5 mouse ovaries, and they are highly sensitive to genotoxic agents, indicating that P5 is an ideal time to study the mechanism by which chemotherapeutic agents induce the death of immature follicles. Thus, in our study, we used P5 female mouse. The mice were intraperitoneally injected with a single dose of Cs (5 mg/kg body weight) as described in a previous study (Gonfloni et al., 2009). Mice in the control group were intraperitoneally injected with the same dose of saline. The treated mice were sacrificed at P9, and their ovaries were fixed. We stained the ovaries and found that the damage induced by Cs was mostly restricted to the primordial follicles (Figure 1A). We counted the numbers of primordial, primary, and secondary follicles (Figure 1B). At this dose of Cs, the number of primordial follicles was reduced to 22.7% of control ovaries. Based on our results and those from previous reports, a dose of 5 mg of Cs per kg body weight can establish the ovarian injury model effectively

in P5 mice. Thus, we administered Cs at a dose of 5 mg/kg body weight in subsequent *in vivo* experiments.

hUCMSC-CM relieves Cs-induced depletion of follicles and preserves fertility

Next, P5 female mice were intraperitoneally injected with a single dose of Cs (5 mg/kg body weight) alone (Cs group) or in combination with hUCMSC-CM (Cs + CM group) to investigate the hUCMSC-CM preservation effects *in vivo*. As a control, two other groups of mice were injected with DMEM/F12 (control group) or hUCMSC-CM (CM group) alone. After 5 days of treatment, we fixed the ovaries and stained the ovarian sections with hematoxylin and eosin (H&E) and DDX4 (Figure 2A). Substantial primordial follicle depletion was observed in the Cs group, whereas an obvious rescue of primordial follicles was observed in the Cs + CM group that was treated with hUCMSC-CM after the Cs injection. We counted the numbers of primordial, primary, and secondary follicles by analyzing the histological sections (Figure 2B). The number of primordial follicles was dramatically decreased in the Cs group compared with the Cs + CM group. Consistent with this finding, we also investigated the protective effect of hUCMSC-CM on follicle reserve in cultured ovaries (Supplementary Figure S1A and B). *In vitro*, hUCMSC-CM protected primordial follicles from depletion when ovaries were exposed to 2 μg/ml Cs. However, hUCMSC-CM did not protect primordial follicles from depletion after the treatment with 4 μg/ml Cs. Therefore, we treated ovaries with 2 μg/ml Cs in subsequent *in vitro* experiments.

P5 mice were injected with a single dose of Cs alone or in combination with hUCMSC-CM to monitor the long-term effects of hUCMSC-CM on ovarian reserve and fertility. hUCMSC-CM was injected daily for 5 days. Pups of the four groups were housed until they were 8 weeks old. Then, we fixed the ovaries and stained the ovarian sections with H&E. Ovaries in the Cs + CM group were smaller than those in control and CM groups, but larger than the Cs group (Figure 2C). Ovaries in the Cs + CM group contained much more growing follicles compared with the Cs group (Figure 2D). In addition, we collected blood samples and measured serum anti-Mullerian hormone (AMH) levels. A higher mean AMH level was detected in the Cs + CM group than in the Cs group (Figure 2E). We also performed breeding test to assess the effects of hUCMSC-CM on fertility. As a result, the number of pups in the Cs group decreased significantly. The mice in the Cs group delivered no pups at round 3 while those in the Cs + CM group can still have pups (Supplementary Figure S1C). These results indicate that hUCMSC-CM partially preserves the ovarian reserve and fertility of mice treated with Cs.

hUCMSC-CM decreases the number of apoptotic cells in cultured ovaries treated with Cs

Next, we focused on the effects of hUCMSC-CM on Cs-induced cell apoptosis. Given the individual difference in drug absorption, we cultured ovaries from P5 mice with 2 μg/ml Cs alone or in combination with hUCMSC-CM. We fixed the ovaries after culture for 6 and 12 h, respectively. Then, we used terminal deoxynucleotidyl transferase dUTP nick end labeling (TUNEL) assay to detect cell apoptosis and counted the number of apoptotic cells from mid-ovary sections. When ovaries were cultured for 6 h, cell apoptosis was slight and the apoptotic cells were granulosa cells (Figure 3A). With the processing of culture, the number of apoptotic cells increased (Figure 3B). In the Cs group, the apoptosis of primordial follicles located at the cortex of the ovary appeared to be obvious. In addition, the apoptosis of granulosa cells was also significant. However, the percentage of TUNEL-positive cells in the Cs + CM group was significantly lower than that in the Cs group (Figure 3B). These observations suggest that hUCMSC-CM can decrease Cs-induced cell apoptosis in the ovaries.

hUCMSC-CM changes the transcriptome patterns of ovaries treated with Cs

Then, we performed RNA-Seq to compare the differentially expressed genes among these groups. We used whole ovaries to perform RNA-Seq. This is because separating granulosa cells and oocytes from ovaries requires a lot of extra time, during which Cs may have induced more severe damage. At the time of 6 h, the protective effects of hUCMSC-CM treatment on ovaries were remarkable, but the negative effects of Cs were relatively inapparent (Figure 4A). The Kyoto Encyclopedia of Genes and Genomes (KEGG) enrichment showed the differentially expressed genes were enriched in the cytokine–cytokine receptor interaction pathway after hUCMSC-CM treatment (Supplementary Figure S2). At the time of 12 h, Cs treatment showed significant negative effects. The results of heatmap showed that the Cs + CM group clustered closer to the control and CM groups, while the Cs group was significantly different (Figure 4B). The differentially expressed genes were enriched in pathways associated with apoptosis, including the PI3K/Akt signaling pathway, MAPK signaling pathway, and p53 pathway (Supplementary Figure S3). As severe cell apoptosis in the Cs group has already happened after Cs treatment for 12 h, we consider that the cell fate has been decided at 12 h. Therefore, to find out the initial factors that influence cell fate decision, we focused on the cytokine–cytokine receptor interaction pathway which was enriched in the earlier stage. Six genes involved in this pathway were verified by quantitative real-time polymerase chain reaction (qRT-PCR) (Figure 5), and the results were consistent with the RNA-Seq data.

G-CSF/PI3K/Akt pathway plays important roles in protecting granulosa cells from apoptosis

Next, we used granulosa cells to further investigate the mechanisms behind the protective effects of hUCMSC-CM. We collected granulosa cells and cultured them with 2 μg/ml Cs alone or in combination with hUCMSC-CM. We found that apoptosis of granulosa cells was significantly decreased in the hUCMSC-CM-treated group (Figure 6A and B; Supplementary Figure S4). G-CSF is beneficial in decreasing follicles loss in an experimental rat model of Cs chemotherapy (Akdemir

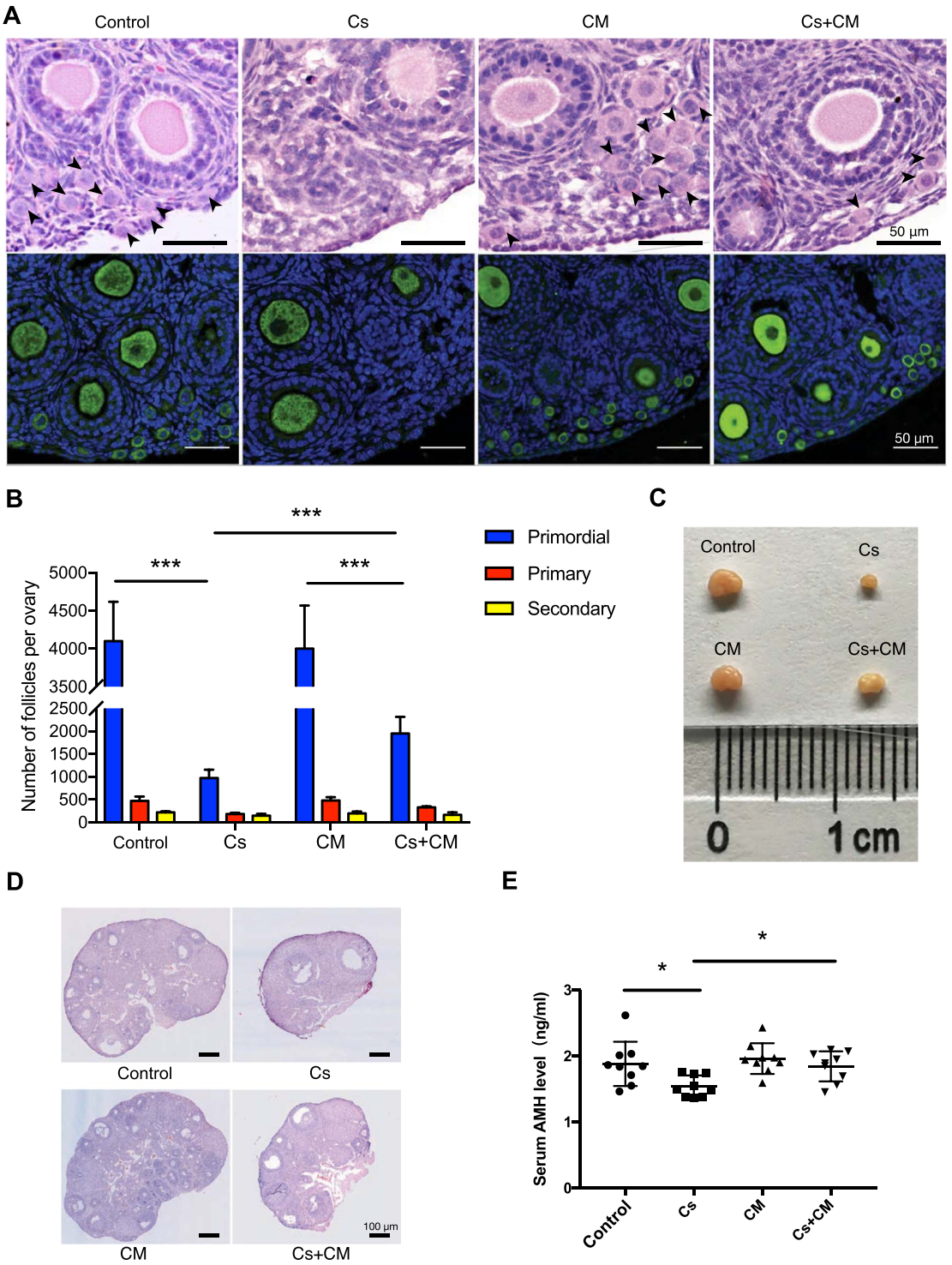

Figure 2 hUCMSC-CM reduces primordial follicle depletion and preserves ovarian reserve and fertility after Cs treatment. (**A**) Analysis of ovarian follicles. Ovary sections used for H&E staining and DDX4 immunofluorescence (cytoplasm, green) were obtained from P9 mice. Cs (5 mg/kg body weight) was administered via intraperitoneal injection at P5 and hUCMSC-CM was injected daily from P5 to P9. Black arrowheads indicate the primordial follicles. Nuclei were stained with DAPI. Scale bar, 50 μm. (**B**) Quantification of the numbers of primordial, primary, and secondary follicles. Data are presented as mean ± SD ($n = 4$). ***$P < 0.001$. (**C**–**E**) Eight-week-old mice were injected with Cs (5 mg/kg body weight) alone or in combination with hUCMSC-CM. (**C**) Gross morphologies of dissected ovaries. (**D**) Images of H&E-stained ovary sections. Scale bar, 100 μm. (**E**) Serum AMH levels in mice ($n = 9$). *$P < 0.05$.

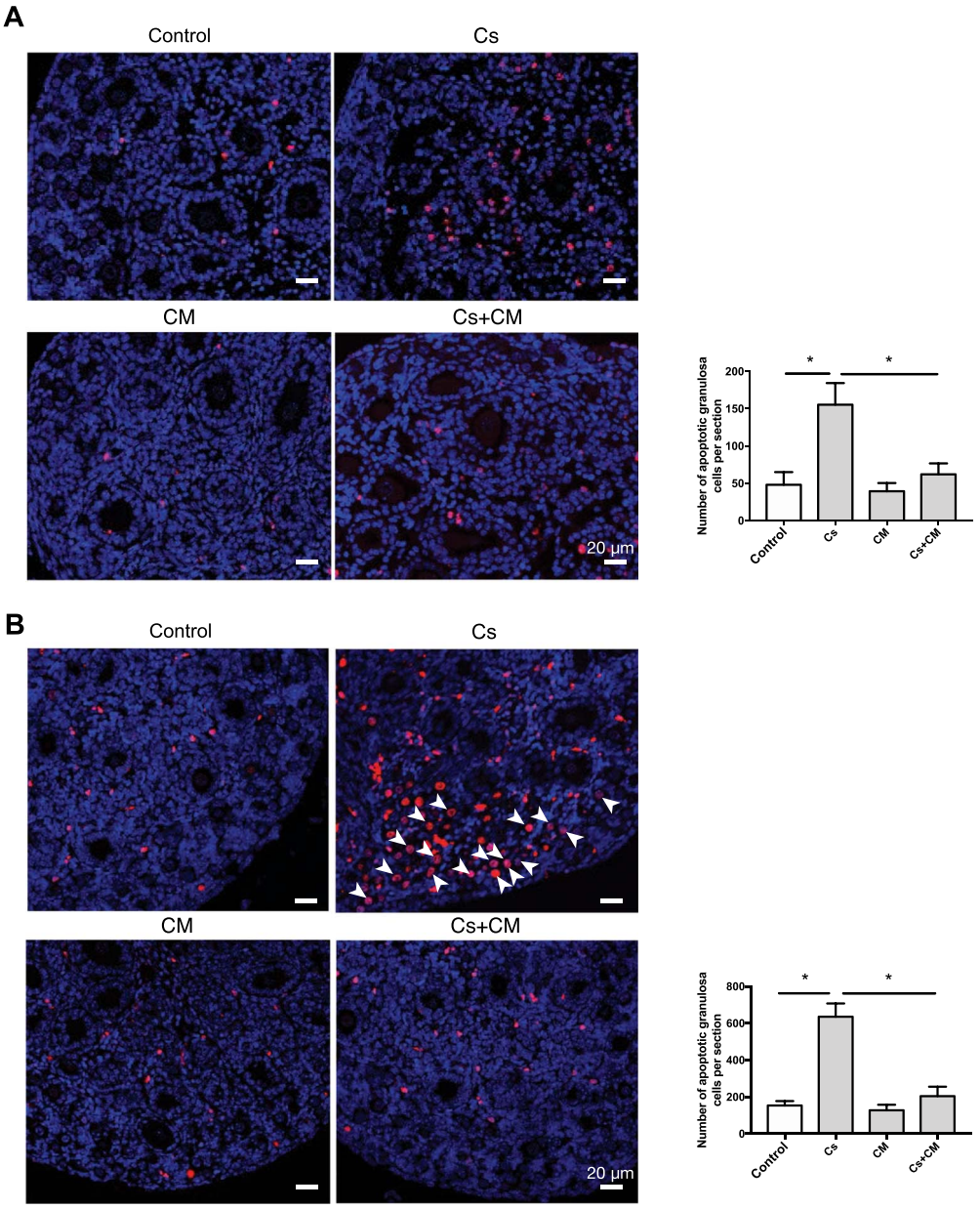

Figure 3 hUCMSC-CM decreases the number of apoptotic cells in cultured ovaries treated with Cs. Images of sections from P5 mouse ovaries stained with TUNEL (red) after treatment with Cs (2 μg/ml) alone or in combination with hUCMSC-CM for 6 h (**A**) or 12 h (**B**). White arrowheads indicate the apoptotic primordial follicles. Nuclei were stained with DAPI. Scale bar, 20 μm. The apoptotic granulosa cells were counted by using ImageJ software. Data are presented as mean ± SD of at least three independent experiments. *$P < 0.05$.

et al., 2014). Moreover, the change in the G-CSF expression level was the most obvious among the differentially expressed genes enriched in the cytokine–cytokine receptor interaction pathway. Thus, we focused on the effects of G-CSF in the present study. We found that the granulosa cells expressed a higher level of G-CSF in the Cs + CM group than in the Cs group, but the expression of G-CSFR, the receptor for G-CSF, showed no significant difference (Figure 6C and D). G-CSF attenuates oxidative stress-induced cell apoptosis through the PI3K/Akt pathway (Kojima et al., 2011). KEGG analysis showed the differentially expressed genes were enriched in the PI3K/Akt pathway at the time of 12 h. Thus, we detected the levels of phosphorylated PI3K and Akt in granulosa cells and found that PI3K and Akt were phosphorylated upon the addition of hUCMSC-CM (Figure 6E). Then, we added recombinant G-CSF to granulosa cells and observed the activation of the PI3K/Akt pathway (Figure 6F). In addition, we transfected granulosa cells with G-CSF siRNA to knock down the expression of G-CSF (Figure 7A). After downregulation of G-CSF, apoptosis of granulosa cells was increased (Figure 7B). When we treated granulosa cells with recombinant G-CSF, both the apoptosis of granulosa cells and the levels of p-PI3K and p-Akt were restored

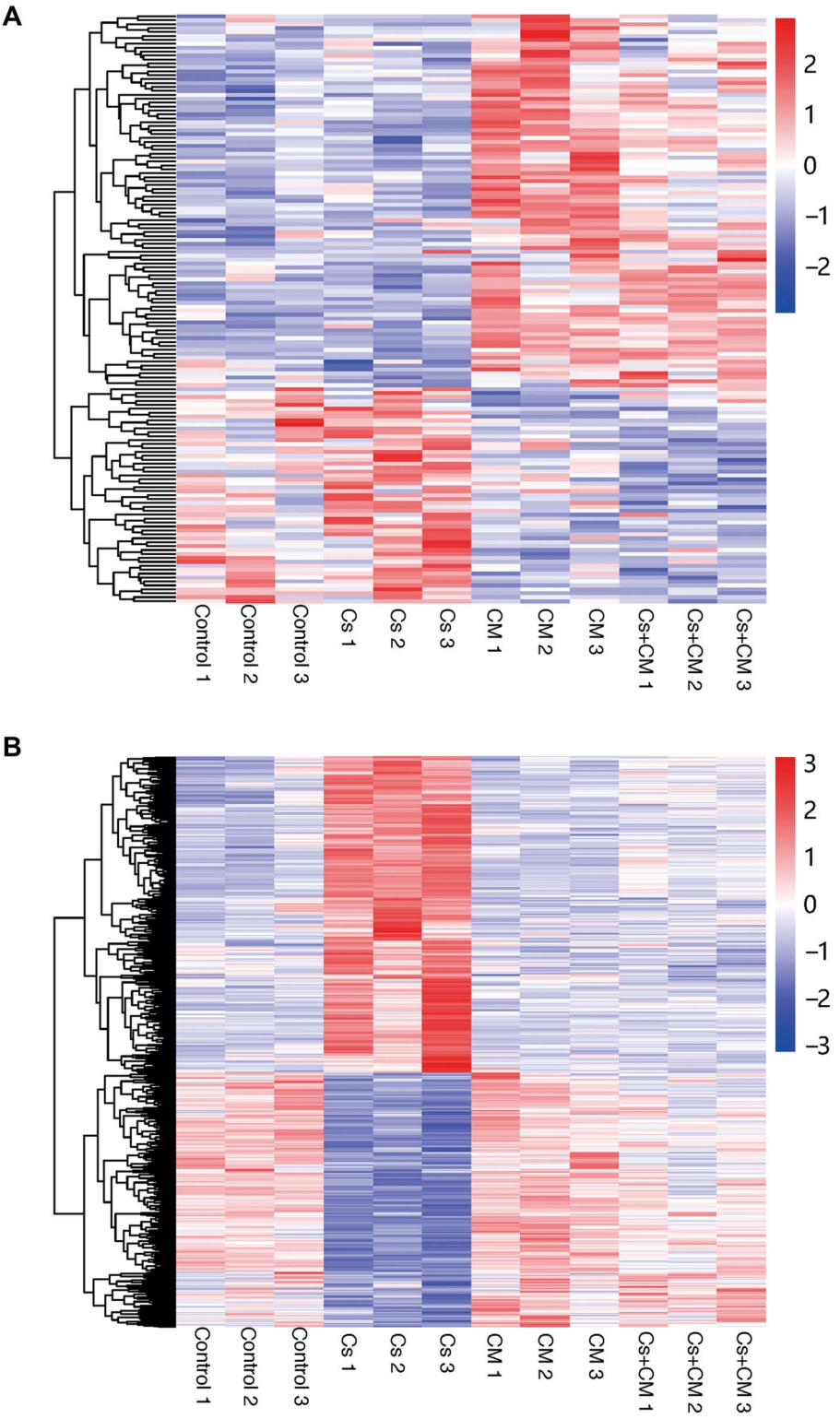

Figure 4 The therapeutic effects of hUCMSC-CM on Cs-damaged ovaries. Heatmap of differentially expressed genes among control, Cs, CM, and Cs + CM groups at the time of 6 h (**A**) or 12 h (**B**).

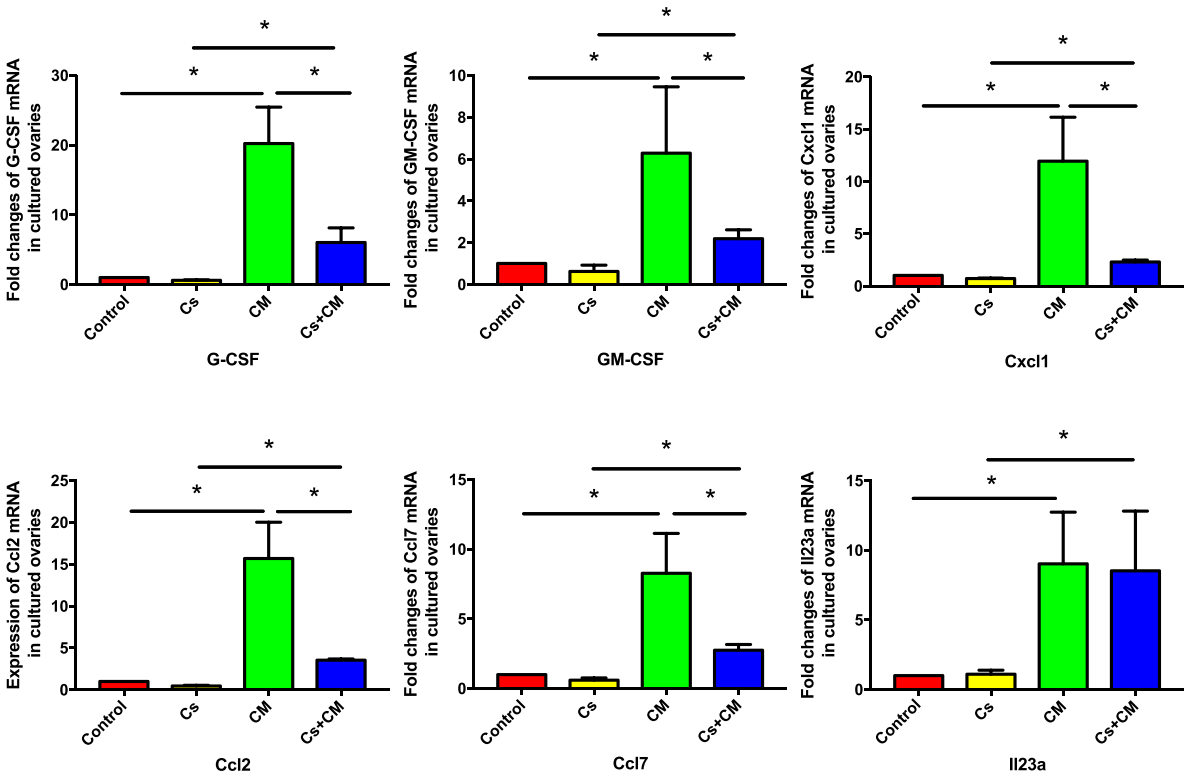

Figure 5 Verification of the expression of G-CSF, GM-CSF, Cxcl1, Ccl2, Ccl7, and Il23a in the ovaries of P5 mice treated with Cs (2 μg/ml) alone or in combination with hUCMSC-CM using qRT-PCR. Data are presented as mean ± SD of at least three independent experiments. $*P < 0.05$.

(Figure 7B and C). Together, these results demonstrate that the G-CSF/PI3K/Akt pathway is important in protecting granulosa cells from apoptosis.

Neutralization of G-CSF abolishes the protective effects of hUCMSC-CM on ovaries

We cultured ovaries from P5 mice with Cs (5 mg/kg body weight) and hUCMSC-CM in the presence or absence of anti-GCSF to confirm the role of G-CSF in mediating the protective effects of hUCMSC-CM on ovaries. The addition of anti-GCSF blocked the protective effects of hUCMSC-CM (Figure 8A). Furthermore, anti-GCSF was administered intraperitoneally to P5 mice to neutralize G-CSF and determine whether G-CSF was involved in protecting ovarian reserve *in vivo*. Cs and hUCMSC-CM were injected intraperitoneally. After 5 days of treatment, primordial follicles in the mice treated with anti-GCSF + Cs + CM decreased more significantly than those treated with Cs + CM or control anti-immunoglobulin G (IgG) (Figure 8B). Taken together, G-CSF is an important factor in mediating the protective roles of hUCMSC-CM on ovaries.

Discussion

Primary ovarian insufficiency (POI) is one of the common disorders in women of reproductive age. Mesenchymal stem cell transplantation has been used as an effective therapy for POI treatment (Yin et al., 2016; Zhang et al., 2018). MSCs have been shown to treat disease by secreting paracrine mediators, including cargo mRNAs, microRNAs, and proteins (Kinnaird et al., 2004; Gnecchi et al., 2005; Timmers et al., 2007; Curley et al., 2012). Here, we confirmed the fertoprotective effects of hUCMSC-CM on Cs-induced ovarian damage in mice.

Recent studies showed that hUCMSC transplantation can reduce cumulus cell apoptosis, restore ovarian function, and increase the levels of sex hormones (Wang et al., 2013; Li et al., 2017). In the present study, we found primordial follicles in the ovaries treated with hUCMSC-CM exhibited an apparent resistance to Cs. Additionally, ovarian reserve and fertility were also preserved after hUCMSC-CM treatment. CM derived from human amniotic epithelial cells (hAECs) can protect ovaries against chemotherapy-induced damage and 109 cytokines in hAEC-CM might participate in apoptosis, angiogenesis, cell cycle, and immune response (Zhang et al., 2017). This study together with ours confirmed the protective effects of MSC-derived CM on ovarian damage, and the work of analyzing the components in hUCMSC-CM is still ongoing in our laboratory.

RNA-Seq was used here to compare the differentially expressed genes of ovaries after hUCMSC-CM and Cs treatments and identify the initial factors mediating the protective effects of hUCMSC-CM. We used whole ovaries for RNA-Seq, which would inevitably result in differentially expressed genes contributed by all the cell types in the ovary. Thus, we detected the expression of the candidate gene before doing further

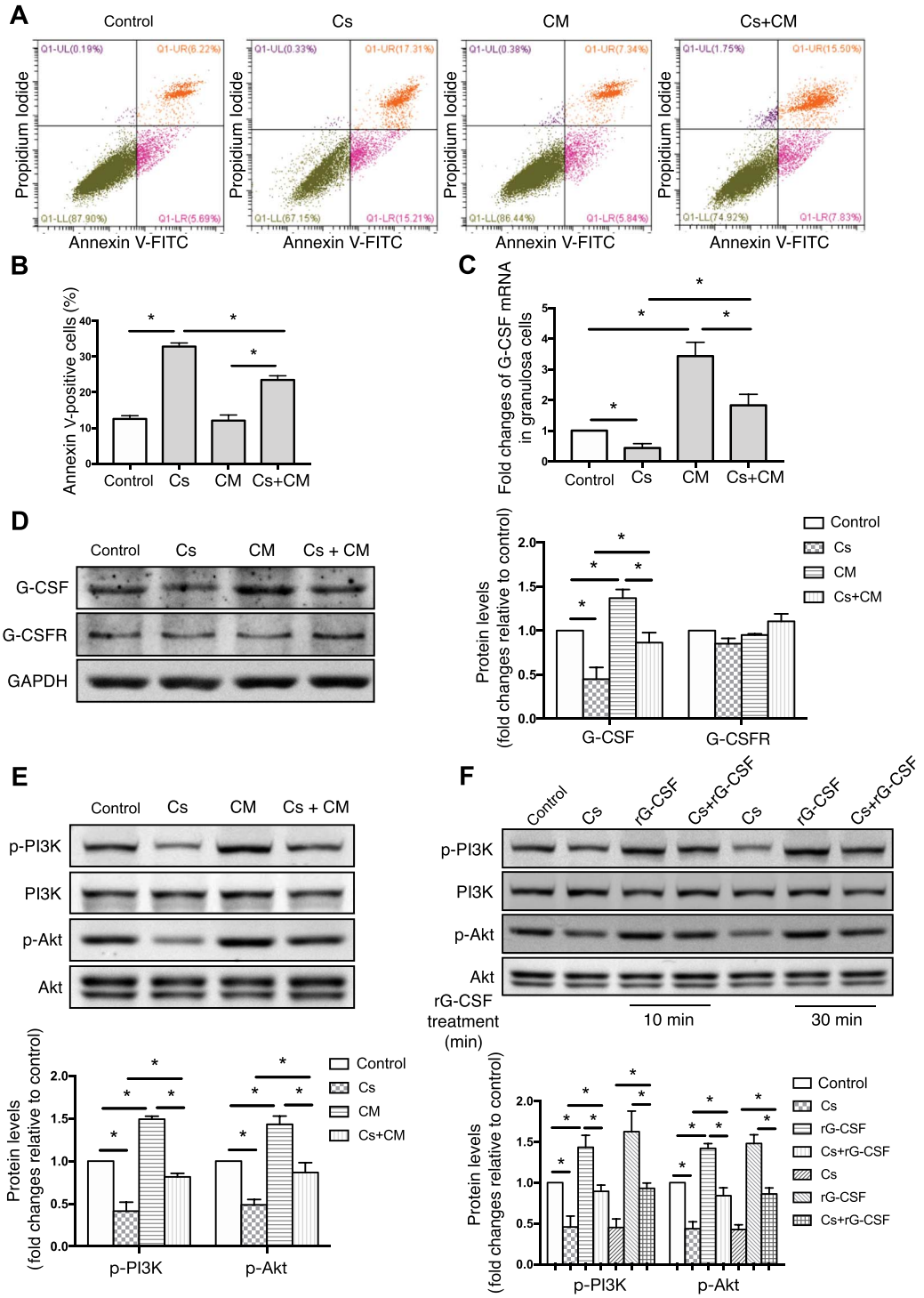

Figure 6 The G-CSF/PI3K/Akt pathway plays important roles in protecting granulosa cells from Cs-induced apoptosis. (**A**–**E**) Granulosa cells were incubated with Cs (2 μg/ml) alone or in combination with hUCMSC-CM for 12 h. (**A**) Flow cytometry analysis of apoptotic granulosa cells. (**B**) The percentages of annexin V-positive cells in four groups. (**C**) qRT-PCR results for G-CSF expression. (**D**) G-CSF and G-CSFR protein levels. (**E**) The levels of phosphorylated PI3K and Akt. (**F**) PI3K and Akt phosphorylation in granulosa cells cultured with or without Cs (2 μg/ml) for 12 h followed by treatment with recombinant G-CSF for specified time. Data are presented as mean ± SD of at least three independent experiments. *$P < 0.05$.

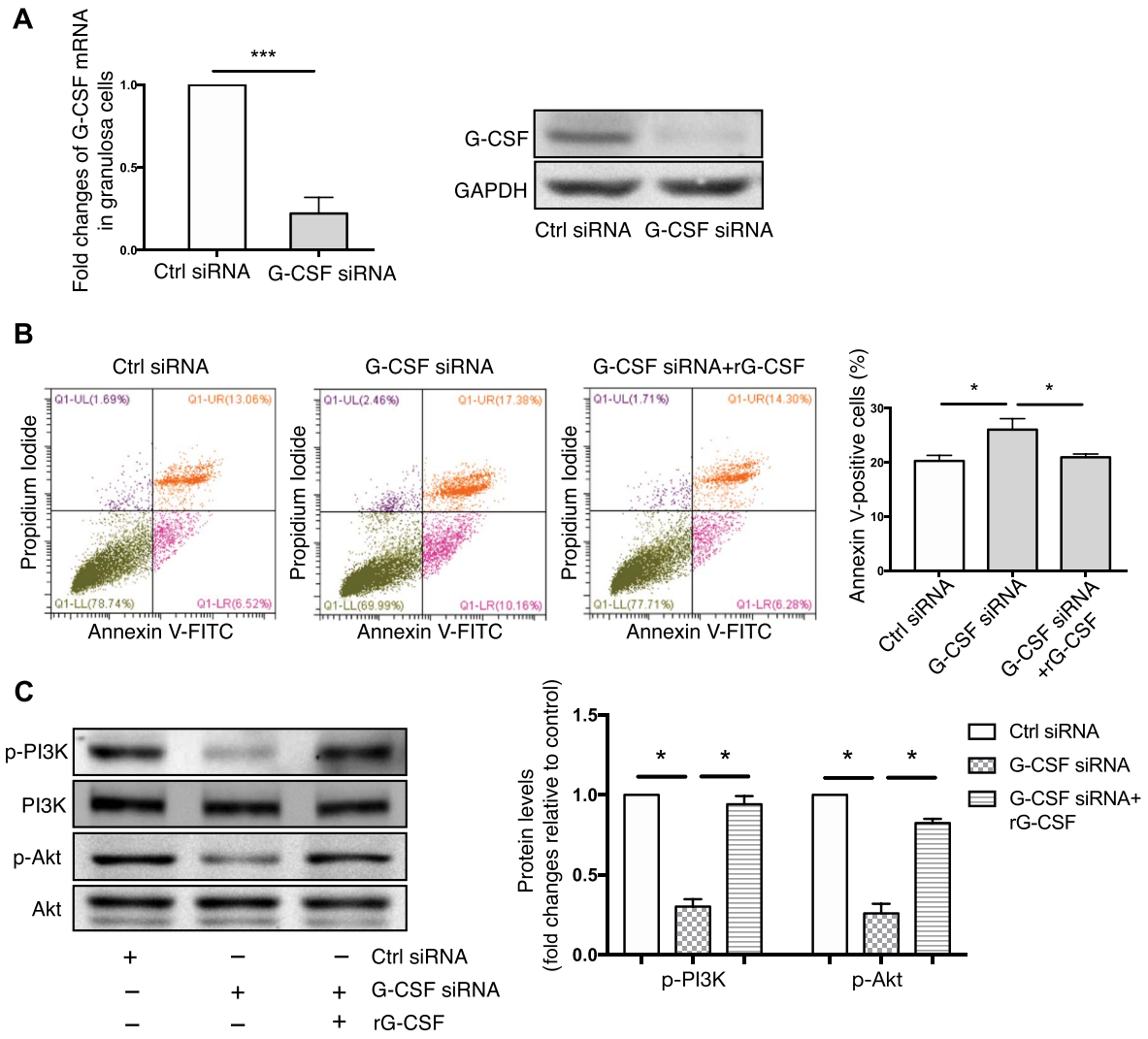

Figure 7 Downregulation of G-CSF increases the apoptosis of granulosa cells. Granulosa cells were transfected for 24 h with G-CSF or control siRNA before treatment with recombinant G-CSF for 24 h. (**A**) qRT-PCR and western blot results of G-CSF in granulosa cells after G-CSF or control siRNA transfection. (**B**) Flow cytometry analysis of apoptotic granulosa cells after recombinant G-CSF treatment. (**C**) PI3K and Akt phosphorylation in granulosa cells after recombinant G-CSF treatment. Data are presented as mean ± SD of at least three independent experiments. $*P < 0.05$.

experiments in granulosa cells. Wang et al. (2013) compared the RNA expression patterns of the ovaries in the hUCMSC transplantation group with the POF model and wild-type control groups using RNA array analysis. They found that the RNA expression pattern in the hUCMSC-treated group was more similar to the wild-type group (Wang et al., 2013). In our study, the RNA expression pattern of the Cs + CM group clustered closer to the control and CM groups, while the Cs group was significantly different at the time of 12 h. The protective effects of hUCMSC-CM were obvious at the time of 6 h. Therefore, we consider that hUCMSC-CM exerts protective effects at the early stage. In order to find out the initial factors that influenced cell fate decision, we focused on earlier stage to select the research target for the following study.

KEGG analysis showed that the differentially expressed genes at the time of 6 h were enriched in cytokine–cytokine receptor interaction pathway. In this pathway, G-CSF, granulocyte-macrophage colony-stimulating factor (GM-CSF), and Ccl2 have been reported as important factors in regulating follicular development and steroidogenic capacity. G-CSF and GM-CSF are glycoproteins produced by many different cell types and have a wide range of physiological functions. G-CSF plays important roles in ovulation, oocyte maturation, development of preimplantation embryos, and trophoblast invasion (Eftekhar et al., 2018). According to Akdemir et al. (2014), G-CSF can reduce follicle loss in a Cs-induced rat model. In the ovary, GM-CSF mRNA and protein synthesis are mainly happened in theca layers and follicular fluid. GM-CSF exerts biological activity through GM-CSF receptor

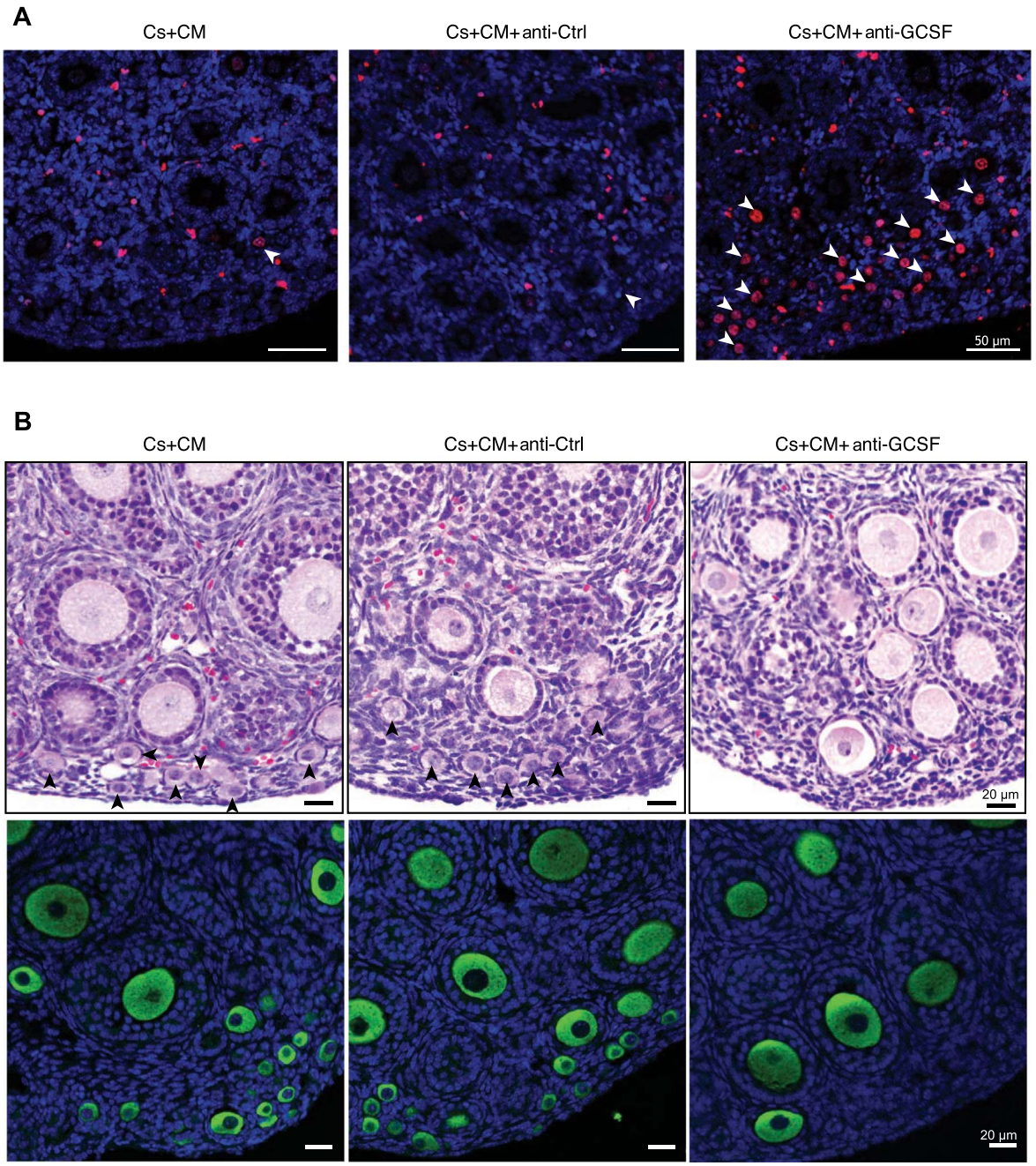

Figure 8 Neutralization of G-CSF abolishes the protective effects of hUCMSC-CM on ovaries. (**A**) Images of sections from P5 mouse ovaries stained with TUNEL (red) after treatment with Cs (2 μg/ml) and hUCMSC-CM in the presence or absence of anti-GCSF for 12 h. White arrowheads indicate the apoptotic primordial follicles. Nuclei were stained with DAPI. Scale bar, 50 μm. (**B**) Ovary sections used for H&E staining and DDX4 immunofluorescence (cytoplasm, green) were obtained from P9 mice. Anti-GCSF was administered via intraperitoneal injection every other day beginning on P4. Cs (5 mg/kg body weight) was administered via intraperitoneal injection on P5, and hUCMSC-CM was injected every other day beginning on P5. Black arrowheads indicate primordial follicles. Nuclei were stained with DAPI. Scale bar, 20 μm. Images are representative of at least three independent experiments.

(Wang et al., 2005). Ccl2 is an important regulatory factor of BMP15 in preventing cumulus cell apoptosis (Zhai et al., 2013). Among these six genes, the fold change of G-CSF expression is most significant. Thus, our study focused on the effects of G-CSF. We found that hUCMSC-CM can upregulate G-CSF expression in granulosa cells and decrease granulosa cell apoptosis. Anti-apoptotic effects of G-CSF were reported in vascular endothelial cells, cardiomyocytes, and neuronal cells (Kojima et al., 2011). KEGG analysis showed that the differentially expressed genes at the time of 12 h were enriched in the PI3K/Akt pathway.

The PI3K/Akt pathway was activated in granulosa cells after the hUCMSC-CM or recombinant G-CSF treatment in the present study. After G-CSF downregulation, recombinant G-CSF restored the levels of p-PI3K and p-Akt. These results indicate that G-CSF is a mediator of hUCMSC-CM in protecting granulosa cells from apoptosis through the PI3K/Akt pathway.

In conclusion, we confirmed that hUCMSCs exert protective effects on Cs-induced ovarian damage via the paracrine pathway. We expect the finding can promote the application of CM in clinical treatment, and we hope infertile patients can benefit from hUCMSC-CM treatment in the future.

Materials and Methods

Animals

CD-1 mice were purchased from SPF Biotechnology Co., Ltd. Mice were housed under standard laboratory conditions in an environmentally controlled room with free access to water and food. Light was provided between 07:00 and 19:00. All procedures involving mice were approved by the Animal Research Committee of the Institute of Zoology, Chinese Academy of Sciences, and the Ethics Committee of Beijing Obstetrics and Gynecology Hospital, Capital Medical University.

Isolation and culture of hUCMSCs

hUCMSCs were provided by Beijing Stem Cell Bank, Institute of Zoology, Chinese Academy of Sciences. Healthy full-term human placental samples were obtained following informed consent. All the samples were used according to the policy of the Ethical Committee of Institute of Zoology, Chinese Academy of Sciences, and the Ethics Committee of Beijing Obstetrics and Gynecology Hospital, Capital Medical University. hUCMSCs were isolated as described previously (Ma et al., 2019). Briefly, umbilical cord tissues were dissected into small segments, and the veins and arteries were removed, following Dulbecco's phosphate-buffered saline (DPBS; Gibco) washing. Then, the umbilical cord segments were cut into small pieces ~0.5–1 mm^3 then cultured in 100-mm plates with SFM (MSCGM-CD; Lonza). The umbilical cord explants were cultured in 37°C and 5% CO_2 humidified atmosphere (Thermo Fisher Scientific); the medium was changed every other day. Cells at passage 4 were utilized for further experiments.

Preparation of hUCMSC-CM

hUCMSCs were cultured in 100-mm plates in DMEM/F12 supplemented with 10% fetal bovine serum (FBS), GlutaMAX, penicillin-G and streptomycin, and basic fibroblast growth factor (all from Gibco). Upon reaching 80% confluence, cells were detached by TrypLE™ Express (Invitrogen) and passaged at the ratio of 1:3. For the collection of hUCMSC-CM, hUCMSCs at passages 4–6 were used. At ~80% confluence, cells were washed three times with phosphate-buffered saline (PBS) and cultured with 6 ml of serum-free DMEM/F12 for 24 h. Afterwards, the culture medium was collected. The supernatant was centrifuged at 1500 rpm for 5 min to remove any cell material, and then the CM were pooled together and used for each experiment.

Animal treatment

P5 CD-1 female mice were intraperitoneally injected with a single dose of Cs (5 mg/kg body weight) (P4394; Merck Millipore) alone as described in a previous study to damage the ovaries (Gonfloni et al., 2009). For hUCMSC-CM treatment, mice were intraperitoneally injected with 30–50 µl hUCMSC-CM daily from P5 to P9 with Microliter Glass Syringe (WPI). No immunoreaction was observed after hUCMSC-CM injection. For G-CSF neutralization, mice were intraperitoneally injected with anti-GCSF (250 µg/kg body weight) (clone 67604; R&D Systems) or control IgG (clone 43414; R&D Systems) every other day from P4 to P9.

Ovary culture

Ovaries were collected from P5 CD-1 mice and cultured in DMEM/F12 or hUCMSC-CM supplemented with 10% FBS, GlutaMAX, penicillin-G and streptomycin, insulin–transferrin–selenium, and 25 µM *N*-acetyl-L-cysteine (A-7250, Merck Millipore) at 37°C in a 5% CO2 atmosphere. Cs was dissolved in normal saline as 1 µg/µl stock solution and added to the medium at the appropriate final concentration.

RNA-Seq analysis

Total RNA was extracted from the whole ovaries using TRIzol reagent (Ambion) prior to transport to Beijing Novogene Co., Ltd, on dry ice. Sequencing libraries were generated using a NEBNext® Ultra™ RNA Library Prep Kit for Illumina® sequencing (NEB) according to the manufacturer's recommendation. The clustering of the index-coded samples was performed on a cBot Cluster Generation System using TruSeq PE Cluster Kit v3-cBot-HS (Illumina) according to the manufacturer's instructions. After cluster generation, the library preparations were sequenced on an Illumina NovaSeq 6000 platform and 125-bp/150-bp paired-end reads were generated. Raw data in the fastq format were uploaded to the NCBI Sequence Read Archive (SRA) under accession number SRP159985. The index of the reference genome was built using STAR, and paired-end clean reads were aligned to the reference genome using STAR (v2.5.1b). Then, the fragment per kilobase of transcript per million mapped reads (FPKM) of each gene were calculated based on the length of the gene and reads count mapped to this gene. The differential expression analysis was performed using the DESeq2 R package (1.10.1). The resulting *P*-values were adjusted using the Benjamini and Hochberg approach to control the false discovery rate. Genes with an adjusted *P*-value < 0.05 identified by DESeq2 were defined as differentially expressed.

Isolation and culture of granulosa cells

Three-week-old CD-1 mice were administered 5 U of pregnant mare serum gonadotropin. After 48 h, the ovaries were collected and granulosa cells were isolated mechanically as described in

a previous study (Couse et al., 2005). Granulosa cells were cultured in DMEM/F12 supplemented with 10% FBS and penicillin-G and streptomycin at 37°C in a 5% CO_2 atmosphere. For recombinant G-CSF treatment, granulosa cells at 70%–80% confluence were treated with 100 ng/ml recombinant G-CSF (Proteintech).

Small interfering RNA transfection

Granulosa cells were transfected with G-CSF small interfering RNA (siRNA) (pool of three pairs, 50 nM each) or control siRNA (RiboBio) using Lipofectamine™ 3000 transfection reagent (Invitrogen) according to the manufacturer's instructions.

Histology

Ovaries were fixed with 4% paraformaldehyde (pH = 7.5) overnight at 4°C then dehydrated and embedded in paraffin. H&E staining was performed using standard histological procedures. The number of follicles in each ovary was estimated using previously described methods (Tilly, 2003). Briefly, paraffin-embedded ovaries were serially sectioned at a thickness of 5 µm. Follicles at primordial, primary, and secondary stages were counted in every fifth section throughout the whole ovary and the mean total number of follicles per section multiplied by the total number of sections of the ovary. Primordial and primary follicles were counted regardless of whether an oocyte nucleus was visible. For secondary follicles, only follicles with a visible oocyte nucleus were counted.

Immunofluorescence staining

For DDX4 foci staining, paraffin-embedded ovary sections were deparaffinized, rehydrated, immersed in a citrate antigen retrieval solution (10 mM), heated in an autoclave, blocked with 3% bovine serum albumin for 1 h at room temperature and then incubated with anti-DDX4 (1:200; #ab-13840; Abcam) overnight at 4°C. The primary antibody was detected by incubating the sections with the corresponding secondary antibody (Invitrogen) at a 1:500 dilution for 1 h at room temperature. Finally, nuclei were stained with 4′,6-diamidino-2-phenylindole (DAPI).

TUNEL assay

An apoptosis detection kit (Vazyme Biotech Co., Ltd) was used for the TUNEL assay according to the manufacturer's instructions. Rehydrated ovary sections were incubated with a 20 µg/ml proteinase K solution for 20 min. Following three 5-min PBS washes, the sections were equilibrated with 1× equilibration buffer for 20 min. Then, terminal deoxynucleotidyl transferase enzyme and the bright red mix were added and incubated for 1 h at 37°C. Finally, nuclei were stained with DAPI. After imaging, TUNEL-positive cells were counted using ImageJ (https://imagej.nih.gov/ij).

RNA extraction and qRT-PCR analysis

Total RNA was extracted by using TRIzol reagent according to the manufacturer's instructions. Total RNA (2 µg) was used for complementary DNA (cDNA) synthesis in a reverse transcription reaction. Oligo (dT) primers were used to synthesize cDNAs, and GAPDH was used for normalization. The cycling parameters were 95°C for 30 sec; 40 cycles of 95°C for 5 sec, 60°C for 20 sec, and 72°C for 15 sec; 95°C for 15 sec; and a final melting step with slow heating from 60°C to 95°C. All reactions were performed in triplicate, and negative control reactions without the reverse transcriptase and template were also performed. Relative gene expression was calculated using the comparative Ct method and the equation $2^{-\Delta\Delta Ct}$ (Livak and Schmittgen, 2001). All primers used for qRT-PCR are listed in Supplementary Table S1.

Western blotting

Western blotting was performed as described by Yang et al. (Yang et al., 2012). Briefly, cells were washed with cold PBS and lysed in radioimmunoprecipitation assay (RIPA) buffer (high) (R0010, Solarbio) containing a protease inhibitor cocktail (P8340, Merck Millipore) and phosphatase inhibitor cocktails II and III (HY-K0022, HY-K0023, MedChem Express). Thirty micrograms of protein were subjected to sodium dodecyl sulfate polyacrylamide gel electrophoresis (SDS–PAGE) followed by electrotransfer onto nitrocellulose membranes. After blocking with 5% skim milk for 1 h, membranes were incubated with primary antibodies against proliferating cell nuclear antigen G-CSF (1:200; #bs-1023R; Bioss), G-CSFR (1:300; #bs-2574R; Bioss), p-PI3K (1:300; #4228; Cell Signaling Technology), PI3K (1:300; #4249; Cell Signaling Technology), p-Akt (1:300; #4060; Cell Signaling Technology), Akt (1:500; #4691; Cell Signaling Technology), or GAPDH (1:2000; #ab22556; Abcam) overnight at 4°C. Membranes were then incubated with horseradish peroxidase-conjugated secondary antibodies (Zhongshan Golden Bridge Biotechnology Co., Ltd) for 1 h at room temperature, and signals were developed using an enhanced chemiluminescence system (Piece). Densitometric quantification was performed using Scion Image software (Scion Corp.).

Flow cytometry analysis

Granulosa cells were collected and washed twice with PBS. Cells were resuspended in 1× binding buffer at a concentration of 1×10^6 cells/ml. The cell suspension (500 µl) was added to a plastic test tube. Next, 5 µl FITC-conjugated annexin V and 10 µl propidium iodide solution were added to each cell suspension. The tubes were incubated at room temperature for exactly 10 min in the dark. The percentage of apoptotic cells was immediately determined with a CytoFLEX flow cytometer (Beckman Coulter), and the data were analyzed using FlowJo software V10.2 (FlowJo).

AMH enzyme-linked immunosorbent assay

The serum AMH level in mice was evaluated using the AMH ELISA kit (Cusabio) according to the manufacturer's instructions. The absorbance was measured at 450 nm, and the serum AMH concentration was calculated. The intra- and inter-assay coefficients of variation were $<15\%$, with a sensitivity of 0.25 ng/ml.

Statistical analysis

Data were collected from at least three different experiments and analyzed using GraphPad Prism 7.0 software. Student's *t*-test was used for comparisons between two groups, and two-way analysis of variance followed by Bonferroni analyses was used for multiple comparisons. Statistical significance was based on the *P*-value: * < 0.05, ** < 0.01, *** < 0.001.

Supplementary material

Supplementary material is available at *Journal of Molecular Cell Biology* online.

Acknowledgements

We are grateful to the Beijing Stem Cell Bank, State Key Laboratory of Reproductive Biology, Institute of Zoology, Chinese Academy of Sciences for providing human hUCMSCs. We thank Shiwen Li, Xili Zhu, and Hua Qin for capturing the histological images and Xia Yang for performing the FACS analysis.

Funding

This work was supported by grants from the National Key Research and Development Program (2017YFA0103800 and 2019YFA0110901), the National Natural Science Foundation of China (81471431, 81871133, 81672085, and 31501102), and Beijing Municipal Administration of Hospitals Clinical Medicine Development of Special Funding Support (ZYLX201830).

Conflict of interest: none declared.

Author contributions: X.Y. and H.W. designed the research; L.H. and L.Y. performed the research; L.H., L.Y., Z.X., S.W., and S.L. analyzed the data; J.H. and W.L. provided human hUCMSCs; L.H., L.Y., H.W., and X.Y. wrote the paper.

References

Akdemir, A., Zeybek, B., Akman, L., et al. (2014). Granulocyte-colony stimulating factor decreases the extent of ovarian damage caused by cisplatin in an experimental rat model. J. Gynecol. Oncol. *25*, 328–333.

Anderson, R.A., and Wallace, W.H.B. (2011). Fertility preservation in girls and young women. Clin. Endocrinol. *75*, 409–419.

Couse, J.F., Yates, M.M., Deroo, B.J., et al. (2005). Estrogen receptor-β is critical to granulosa cell differentiation and the ovulatory response to gonadotropins. Endocrinology *146*, 3247–3262.

Curley, G.F., Hayes, M., Ansari, B., et al. (2012). Mesenchymal stem cells enhance recovery and repair following ventilator-induced lung injury in the rat. Thorax *67*, 496–501.

Del, M.L., Boni, L., Michelotti, A., et al. (2011). Effect of the gonadotropin-releasing hormone analogue triptorelin on the occurrence of chemotherapy-induced early menopause in premenopausal women with breast cancer: a randomized trial. JAMA *306*, 269–276.

Donnez, J., and Dolmans, M. (2011). Preservation of fertility in females with haematological malignancy. Brit. J. Haematol. *154*, 175–184.

Eftekhar, M., Naghshineh, E., and Khani, P. (2018). Role of granulocyte colony-stimulating factor in human reproduction. J. Res. Med. Sci. *23*, 7.

Gerber, B., von, G., Stehle, H., et al. (2011). Effect of luteinizing hormone-releasing hormone agonist on ovarian function after modern adjuvant breast cancer chemotherapy: the GBG 37 ZORO study. J. Clin. Oncol. *29*, 2334–2341.

Gnecchi, M., He, H., Liang, O.D., et al. (2005). Paracrine action accounts for marked protection of ischemic heart by Akt-modified mesenchymal stem cells. Nat. Med. *11*, 367–368.

Gonfloni, S., Di, L., Caldarola, S., et al. (2009). Inhibition of the c-Abl–TAp63 pathway protects mouse oocytes from chemotherapy-induced death. Nat. Med. *15*, 1179–1185.

Jia, Y., Shi, X., Xie, Y., et al. (2017). Human umbilical cord stem cell conditioned medium versus serum-free culture medium in the treatment of cryopreserved human ovarian tissues in in-vitro culture: a randomized controlled trial. Stem Cell Res. Ther. *8*, 152.

Khanmohammadi, N., Sameni, H.R., Mohammadi, M., et al. (2018). Effect of transplantation of bone marrow stromal cell-conditioned medium on ovarian function, morphology and cell death in cyclophosphamide-treated rats. Cell J. *20*, 10–18.

Kim, H.O., Choi, S., and Kim, H. (2013a). Mesenchymal stem cell-derived secretome and microvesicles as a cell-free therapeutics for neurodegenerative disorders. Tissue Eng. Regen. Med. *10*, 93–101.

Kim, S.Y., Cordeiro, M.H., Serna, V.A., et al. (2013b). Rescue of platinum-damaged oocytes from programmed cell death through inactivation of the p53 family signaling network. Cell Death Differ. *20*, 987–997.

Kinnaird, T., Stabile, E., Burnett, M.S., et al. (2004). Local delivery of marrow-derived stromal cells augments collateral perfusion through paracrine mechanisms. Circulation *109*, 1543–1549.

Kojima, H., Otani, A., Oishi, A., et al. (2011). Granulocyte colony-stimulating factor attenuates oxidative stress-induced apoptosis in vascular endothelial cells and exhibits functional and morphologic protective effect in oxygen-induced retinopathy. Blood *117*, 1091–1100.

Letourneau, J.M., Ebbel, E.E., Katz, P.P., et al. (2012). Acute ovarian failure underestimates age-specific reproductive impairment for young women undergoing chemotherapy for cancer. Am. Cancer Soc. *118*, 1933–1939.

Li, J., Mao, Q., He, J., et al. (2017). Human umbilical cord mesenchymal stem cells improve the reserve function of perimenopausal ovary via a paracrine mechanism. Stem Cell Res. Ther. *8*, 55.

Livak, K.J., and Schmittgen, T.D. (2001). Analysis of relative gene expression data using real-time quantitative PCR and the $2^{-\Delta\Delta C_T}$ method. Methods *25*, 402–408.

Ma, J., Wu, J., Han, L., et al. (2019). Comparative analysis of mesenchymal stem cells derived from amniotic membrane, umbilical cord, and chorionic plate under serum-free condition. Stem Cell Res. Ther. *10*, 19.

Mohr, A., and Zwacka, R. (2018). The future of mesenchymal stem cell-based therapeutic approaches for cancer—from cells to ghosts. Cancer Lett. *414*, 239–249.

Morgan, S., Anderson, R.A., Gourley, C., et al. (2012). How do chemotherapeutic agents damage the ovary? Hum. Reprod. Update *18*, 525–535.

Morita, Y., and Tilly, J.L. (2000). Sphingolipid regulation of female gonadal cell apoptosis. Ann. NY Acad. Sci. *905*, 209–220.

Pawitan, J.A. (2014). Prospect of stem cell conditioned medium in regenerative medicine. Biomed. Res. Int. *2014*, 1–14.

Phinney, D.G., and Pittenger, M.F. (2017). Concise review: MSC-derived exosomes for cell-free therapy. Stem Cells *35*, 851–858.

Rossi, V., Lispi, M., Longobardi, S., et al. (2017). LH prevents cisplatin-induced apoptosis in oocytes and preserves female fertility in mouse. Cell Death Differ. *24*, 72–82.

Sassarini, J., Lumsden, M.A., and Critchley, H.O.D. (2015). Sex hormone replacement in ovarian failure—new treatment concepts. Best Pract. Res. Cl. En. *29*, 105–114.

Sdrimas, K., and Kourembanas, S. (2014). MSC microvesicles for the treatment of lung disease: a new paradigm for cell-free therapy. Antioxid. Redox Sign. *21*, 1905–1915.

Sheikhansari, G., Aghebati-Maleki, L., Nouri, M., et al. (2018). Current approaches for the treatment of premature ovarian failure with stem cell therapy. Biomed. Pharmacother. *102*, 254–262.

Tilly, J.L. (2003). Ovarian follicle counts—not as simple as 1, 2, 3. Reprod. Biol. Endocrinol. *1*, 11.

Timmers, L., Lim, S.K., Arslan, F., et al. (2007). Reduction of myocardial infarct size by human mesenchymal stem cell conditioned medium. Stem Cell Res. *1*, 129–137.

Volarevic, V., Bojic, S., Nurkovic, J., et al. (2014). Stem cells as new agents for the treatment of infertility: current and future perspectives and challenges. Biomed. Res. Int. *2014*, 1–8.

Wang, H., Wen, Y., Polan, M.L., et al. (2005). Exogenous granulocyte-macrophage colony-stimulating factor promotes follicular development in the newborn rat in vivo. Hum. Reprod. *20*, 2749–2756.

Wang, S., Yu, L., Sun, M., et al. (2013). The therapeutic potential of umbilical cord mesenchymal stem cells in mice premature ovarian failure. Biomed. Res. Int. *2013*, 690491.

Wang, Z., Wang, Y., Yang, T., et al. (2017). Study of the reparative effects of menstrual-derived stem cells on premature ovarian failure in mice. Stem Cell Res. Ther. *8*, 11.

Waxman, J.H., Ahmed, R., Smith, D., et al. (1987). Failure to preserve fertility in patients with Hodgkin's disease. Cancer Chemother. Pharmacol. *19*, 159–162.

Webber, L., Davies, M., Anderson, R., et al. (2016). ESHRE Guideline: management of women with premature ovarian insufficiency. Hum. Reprod. *31*, 926–937.

Yang, X., Zhou, Y., Peng, S., et al. (2012). Differentially expressed plasma microRNAs in premature ovarian failure patients and the potential regulatory function of mir-23a in granulosa cell apoptosis. Reproduction *144*, 235–244.

Yin, N., Zhao, W., Luo, Q., et al. (2016). Restoring ovarian function with human placenta-derived mesenchymal stem cells in autoimmune-induced premature ovarian failure mice mediated by treg cells and associated cytokines. Reprod. Sci. *25*, 1073–1082.

Zhai, B., Liu, H., Li, X., et al. (2013). BMP15 prevents cumulus cell apoptosis through CCL2 and FBN1 in porcine ovaries. Cell. Physiol. Biochem. *32*, 264–278.

Zhang, H., Luo, Q., Lu, X., et al. (2018). Effects of hPMSCs on granulosa cell apoptosis and AMH expression and their role in the restoration of ovary function in premature ovarian failure mice. Stem Cell Res. Ther. *9*, 20.

Zhang, Q., Bu, S., Sun, J., et al. (2017). Paracrine effects of human amniotic epithelial cells protect against chemotherapy-induced ovarian damage. Stem Cell Res. Ther. *8*, 270.